

# Topological, Geometric, and Chemical Order in Materials: Insights from Solid-State NMR

DOMINIQUE MASSIOT,\* ROBERT J. MESSINGER,  
SYLVIAN CADARS, MICHAËL DESCHAMPS,  
VALERIE MONTOUILLOUT, NADIA PELLERIN,  
EMMANUEL VERON, MATHIEU ALLIX, PIERRE FLORIAN, AND  
FRANCK FAYON

CNRS, CEMHTI, UPR 3079, F-45071, Orléans, France, and  
University of Orléans, CEMHTI, UPR CNRS 3079, F-45071,  
Orléans, France

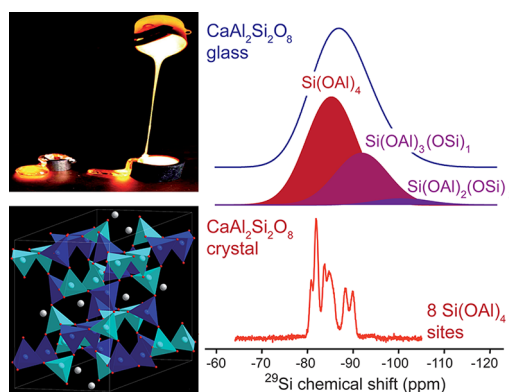
RECEIVED ON DECEMBER 17, 2012

## CONSPECTUS

Unlike the long-range order of ideal crystalline structures, local order is an intrinsic characteristic of real materials and often serves as the key to the tuning of their properties and their final applications. Although researchers can easily assess local ordering using two-dimensional imaging techniques with resolution that approaches the atomic level, the diagnosis, description, and qualification of local order in three dimensions is much more challenging.

Solid-state nuclear magnetic resonance (NMR) and its panel of continually developing instruments and methods enable the local, atom-selective characterization of structures and assemblies ranging from the atomic to the nanometer length scales. By making use of the indirect  $J$ -coupling that distinguishes chemical bonds, researchers can use solid-state NMR to characterize a variety of materials, ranging from crystalline compounds to amorphous or glassy materials. In crystalline compounds showing some disorder, we describe and distinguish the contributions of topology, geometry, and local chemistry in ways that are consistent with X-ray diffraction and computational approaches. We give examples of materials featuring either chemical disorder in a topological order or topological disorder with local chemical order. For glasses, we show that we can separate geometric and chemical contributions to the local order by identifying structural motifs with a viewpoint that extends from the atomic scale up to the nanoscale.

As identified by solid state NMR, the local structure of amorphous materials or glasses consists of well-identified structural entities up to at least the nanometer scale. Instead of speaking of disorder, we propose a new description for these structures as a continuous assembly of locally defined structures, an idea that draws on the concept of locally favored structures (LFS) introduced by Tanaka and coworkers. This idea provides a comprehensive picture of amorphous structures based on fluctuations of chemical composition and structure over different length scales. We hope that these local or molecular insights will allow researchers to consider key questions related to nucleation and crystallization, as well as chemically (spinodal decomposition) or density-driven (polyamorphism) phase separation, which could lead to future applications in a variety of materials.



## Introduction

Real crystalline materials usually feature some amount of disorder, whether in their bulk structures or at their surfaces and interfaces, where the extent of local disordering often imparts unique properties to the material. Perfectly ordered crystal structures are considered as references and the concept of *disorder* implies a departure from order that cannot always

be defined *a priori*. Conversely, amorphous materials often exhibit short-range order, such as nanoscale structural motifs, clustering, or local ordering at the level of the atomic coordination sphere. Describing this short-range order is crucial for understanding the origins of their material properties.

Order and disorder are easier to visualize in two-dimensional (2D) objects, where direct-imaging techniques

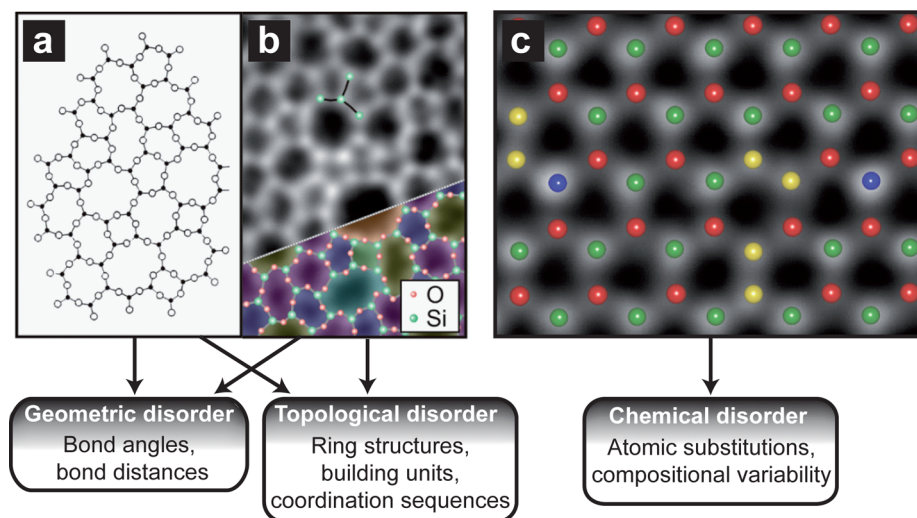


**FIGURE 1.** (a) Historical 2D sketch of an amorphous SiO<sub>2</sub> network.<sup>2</sup> (b) Atomic-resolution image of a silica film showing a topologically and geometrically disordered network of tetrahedra.<sup>1</sup> (c) Boron nitride sheet exhibiting chemical disorder in a topologically and geometrically ordered hexagonal network.<sup>3</sup> The regular arrangement of boron (red) and nitrogen atoms (green) is locally substituted by oxygen (blue) or carbon (yellow). Adapted from refs 1 (copyright 2012 American Chemical Society) and 3 (copyright 2010 Nature Publishing Group) with authorization.

enable atomic-level resolution. For example, a disordered bilayer film of silica (SiO<sub>2</sub>) deposited on a metallic surface (Figure 1b<sup>1</sup>) features topological disorder (distribution of ring sizes) and geometric disorder (distribution of bond angles and distances) within a chemically homogeneous material. Remarkably, it is closely comparable to the historical 2D sketch of the *continuous random network* introduced by Zachariasen in the early 1930s<sup>2,1</sup> (Figure 1a). Figure 1c shows the counterpart of the previous example where a boron nitride sheet with a topologically and geometrically ordered hexagonal network exhibits chemical disorder related to oxygen or carbon substitutional defects.<sup>3</sup> Interestingly, both structural and chemical heterogeneity at the nanometer scale are combined in the *modified random network* of Greaves,<sup>4</sup> a reference picture for the structures of oxide glasses. Topological, geometric, and chemical orders are thus all entangled in the structures of both crystalline and amorphous materials, involving *locally ordered structures* that are usually described as defects, substitutions, and combinations of order and disorder over different length scales.

The latest generation of solid-state NMR experiments extends far beyond distinguishing between the different chemical environments of the selectively observed atoms. They allow the characterization of larger ensembles of atoms through correlation, spectral editing, or spin counting experiments that selectively probe spatial proximities from dipolar interactions or chemical bonds from indirect *J*-couplings. Correlation experiments allow interacting spins to be identified, quantitative analyses of magnetization build-up

curves or *J*-resolved experiments yield measurements of spin–spin couplings, and multiple-quantum filtering allows spectral editing of selected spin ensembles. We shall show how such experiments can disentangle chemical and geometric order, enabling local structural motifs to be identified up to the nanometer scale. These methods open the possibility to switch from the crystallographic *average* long-range description of material structures to a direct description of local order from the atomic to nanometer scales.

## Disorder in Crystalline Structures

The structures of crystalline compounds are described as the repetition of a basic unit cell built from a minimal set of atomic positions using symmetry operations. These parameters may be determined with extremely high levels of precision from neutron or synchrotron diffraction data. However, such techniques only reflect an *average* long-range structure, making local chemical or geometric disorder challenging to characterize. While current diffraction techniques may capture deviations from ideal structures, introducing modulations or identifying occupancy factors and anisotropic atomic displacements, solid-state NMR techniques can often probe the degree and type of local order.

**Chemical Disorder in a Crystalline Structure.** The gehlenite [Ca<sub>2</sub>Al<sub>2</sub>SiO<sub>7</sub>]<sup>5</sup> compound is a calcium aluminosilicate whose structure allows substitution of Ca by rare-earth elements leading to “a laser material intermediate between ordered crystals and glasses”.<sup>6</sup> Its peculiar “disordered” character, present even in single crystals, originates from Si/Al

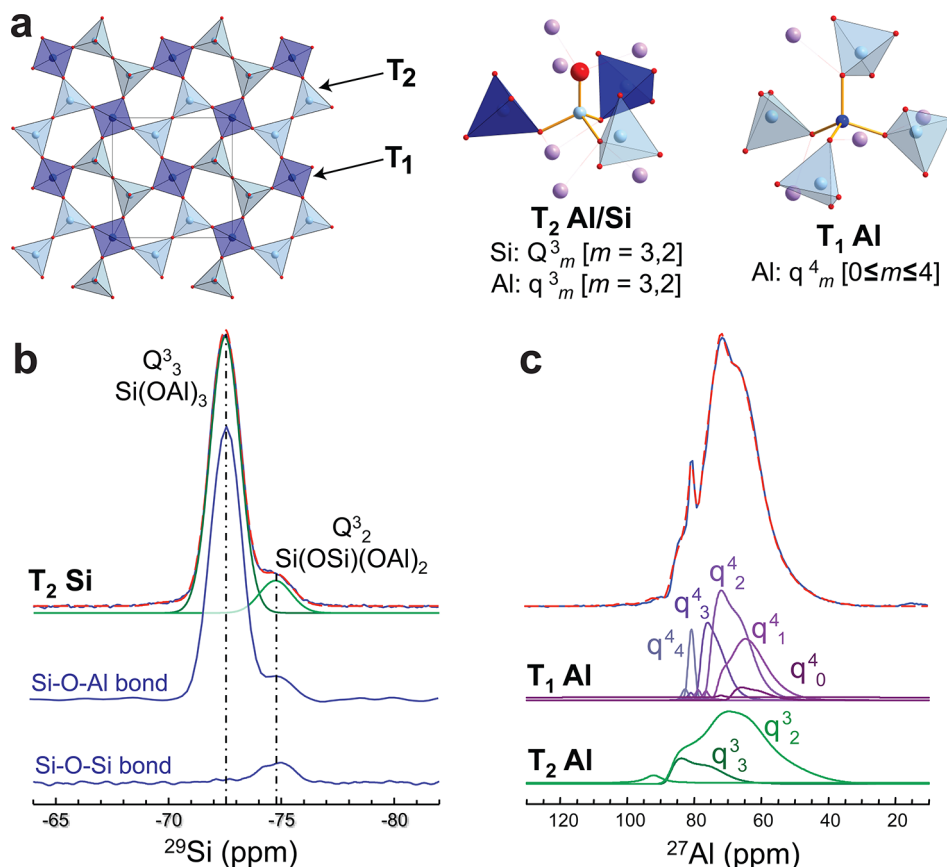


**FIGURE 2.** (a) Schematic representation of the gehlenite  $\text{Ca}_2\text{Al}_2\text{SiO}_7$  structure.  $T_1$  and  $T_2$  sites are dark and light tetrahedra, respectively. (b)  $^{29}\text{Si}$  and (c)  $^{27}\text{Al}$  quantitative single-pulse MAS NMR spectra. The individual contributions were obtained from Al/Si and Si/Si pair filtering experiments for  $^{29}\text{Si}$  (b) and from MQ-MAS and Al/ $n$ Si multiple-quantum filtering<sup>5</sup> for  $^{27}\text{Al}$  (c).

substitution within one of the distinct crystallographic tetrahedral sites of the well-defined average crystalline structure.<sup>7</sup> Gehlenite structure (Figure 2a) consists of alternating layers of (Si,Al) $\text{O}_4$  tetrahedra and Ca atoms stacking along the  $c$ -axis. The composition of the (Si,Al) $\text{O}_4$  layers may be described by using  $Q_m^n$  or  $q_m^n$  notation for tetrahedral Si and Al, respectively, where  $n$  is the number of bridging oxygen atoms and  $m$  is the number of bonded  $\text{AlO}_4$  units ( $0 \leq m \leq n \leq 4$ ). They feature  $T_1$  sites, fully occupied by aluminum ( $q_m^4$ ), and  $T_2$  sites, occupied either by Si ( $Q_m^3$ ) or by Al atoms ( $q_m^3$ ). The different distributions of Si and Al atoms in the  $T_2$  sites (Figure 2a) result in a range of different possible chemical environments: two for silicon ( $T_2 Q_m^3$ ,  $m = 3, 2$ ) and seven for aluminum ( $T_1 q_m^4$ ,  $0 \leq m \leq 4$ , and  $T_2 q_m^3$ ,  $m = 3$  or  $2$ ), which cannot be disentangled in the average long-range structure (Figure 2a).

Quantitative  $^{29}\text{Si}$  and  $^{27}\text{Al}$  magic-angle-spinning (MAS) NMR experiments, in combination with spectral editing NMR experiments that select groups of Si or Al atoms, enable the identification of the signatures of different  $T_1$  and  $T_2$  sites. The  $^{29}\text{Si}$  MAS NMR spectrum shows two components

that can be unambiguously assigned using a multiple-quantum (MQ)-filtered experiment that selects the pairs of chemically bonded silicon atoms ( $^{29}\text{Si}-\text{O}-^{29}\text{Si}$ ) and thus only retains contributions from  $Q_2^3$  motifs (Figure 2b).

The relative proportion of these two Si environments is a direct measurement of the extent of violation of the “Loewenstein” rule<sup>8</sup> that states that linkages between  $\text{AlO}_4$  tetrahedra are energetically unfavorable in aluminosilicates. Moreover, while the different  $^{29}\text{Si}$  NMR resonances are an order of magnitude broader than those usually found in crystalline silicates, the Si–O–Si bond angle distribution of  $136.5 \pm 0.4^\circ$  determined from measurements of  $^2J_{\text{Si}-\text{O}-\text{Si}}$  couplings<sup>12</sup> is characteristic of crystalline silicates. These results establish the superposition of a dominant chemical disorder and a small geometric disorder.

The  $^{27}\text{Al}$  MAS NMR spectra are rendered complex by the broadening due to the quadrupolar nature of  $^{27}\text{Al}$ . Examination of high-resolution MQ-MAS and quantitative single-pulse experiments performed at two different magnetic fields (9.4 and 17.6 T), together with spectral editing experiments that select Al with different numbers of Al–O–Si

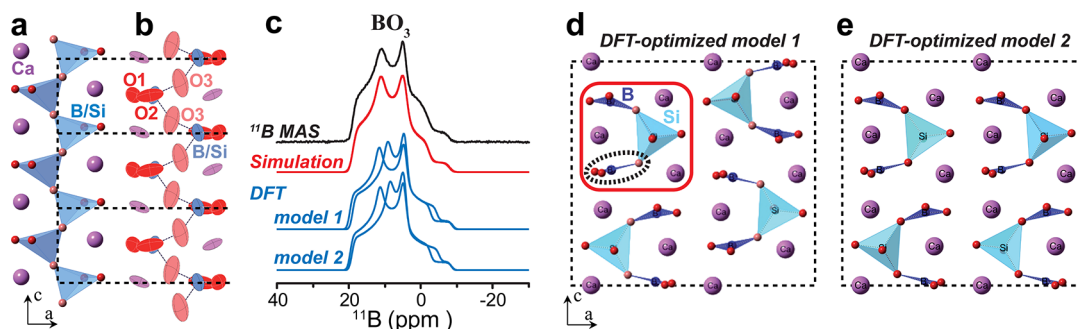


**FIGURE 3.** (a) Chains of distorted  $\text{TO}_4$  tetrahedra in the average long-range structure of  $\text{CaSi}_{1/3}\text{B}_{2/3}\text{O}_{8/3}$ . (b) The fractional occupancy of B/Si atoms in  $\text{TO}_4$  sites is reflected in the O3 ellipsoids. (c)  $^{11}\text{B}$  MAS NMR spectrum indicating presence of  $\text{BO}_3$  units. (d, e) Two DFT-optimized models consisting of  $1 \times 1 \times 3$  supercells both built with an identical basic unit (highlighted in red) but in a different topological arrangement.<sup>9</sup>

bonds (multiple-quantum filtering) allows the reliable determination of the NMR parameters of the seven chemically distinct aluminum environments (Figure 2c), showing a decrease of  $-3$  ppm of the  $^{27}\text{Al}$  isotropic chemical shift for each substitution of aluminum by silicon in the coordination sphere of the observed aluminum.

The measured NMR parameters and their distributions are related to the structure by means of quantum chemical density functional theory (DFT)-based computations using periodic boundary conditions.<sup>5</sup> The atomic positions in a supercell were optimized with  $\text{T}_2$  sites filled with Al or Si atoms distributed either randomly or in compliance with the “Loewenstein” exclusion rule.<sup>8</sup> The calculations show that the geometric disorder depends upon the local chemical order, where the “random” filling induces a broader distribution of parameters and confirms that the  $^{27}\text{Al}$  isotropic chemical shifts of the  $q_m^n$  tetrahedra depend linearly on  $m$ .

The example of gehlenite illustrates the unique capability of advanced solid-state NMR methods to identify the various local environments and the nature of their distributions, which are directly linked to the local chemical disorder and moderate extents of geometric disorder in an otherwise topologically ordered network of tetrahedra.

**Topological Disorder in a Crystalline Structure.** The structure of the  $\text{CaSi}_{1/3}\text{B}_{2/3}\text{O}_{8/3}$  calcium borosilicate has been recently characterized by transmission electron microscopy coupled to Rietveld refinements of neutron and synchrotron powder diffraction data.<sup>9</sup> Its average long-range structure consists of an array of linear chains of  $\text{TO}_4$  tetrahedra (Figure 3a) in the form of a mixed composition of  $1/3$  Si and  $2/3$  B for the T sites and a partial occupancy of  $2/3$  for the bridging oxygen sites (O3, Figure 3b). From the *average* structure, the  $\text{TO}_4$  tetrahedra appear to be severely distorted and to deviate from a perfectly ordered structure, because they exhibit large and anisotropic atomic displacements.

A one-dimensional  $^{11}\text{B}$  MAS solid-state NMR experiment sheds light onto the local structure (Figure 3c). The line shape is characteristic of planar  $\text{BO}_3$  units, each associated with an oxygen vacancy and thus interrupting the chain. The average chain of  $\text{TO}_4$  sites thus consists of an arrangement of  $\text{SiO}_4$  tetrahedra and  $\text{BO}_3$  planar units in a 1:2 ratio, and the atomic displacements reflect the average view of the structure. The increased spectral resolution provided by 2D MQ-MAS experiments (not shown) reveals that B–O–B chemical bonds are excluded, which implies that the structure is composed solely of  $\text{Ca}_3\text{B}_2\text{SiO}_8$  ( $\text{B}^{\text{III}}-\text{O}-\text{Si}^{\text{IV}}-\text{O}-\text{B}^{\text{III}}$ ) units.<sup>9</sup>

The simplest structural models characteristic of  $\text{CaSi}_{1/3}\text{B}_{2/3}\text{O}_{8/3}$  must thus consist of  $\text{Ca}_3\text{B}_2\text{SiO}_8$  building units arranged in multiple unit cells of the *average* structure, leading to at least two possible topological arrangements of the building units (Figure 3d,e). DFT methods allow (i) the optimization of the geometry of these two models and (ii) the computation of their  $^{11}\text{B}$  NMR signatures (isotropic chemical shift and EFG tensor). Remarkably the two models, involving similar  $\text{Ca}_3\text{B}_2\text{SiO}_8$  units, yield very similar  $^{11}\text{B}$  signatures that are both compatible with the observed spectrum. In reality, the material likely consists of combinations of different topologies of the interchain arrangements at the scale of tens of nanometers. Indeed, nanoscale ordered domains, exhibiting superstructures, are observed in high-resolution electron microscopy images.<sup>9</sup>

**Chemical Disorder in Layered Materials.** Layered materials, such as clay minerals or layered double hydroxides (LDHs), have been widely studied for their applications in catalysis, in drug delivery, or as a waste barrier.<sup>10</sup> These materials often feature chemical disorder that remains challenging to describe in an average long-range structure due to the stacking disorder between sheets. For example, the distribution of  $\text{Mg}^{2+}$  and  $\text{Al}^{3+}$  cations within a single layer of hexagonally arranged octahedral sites of LDHs has

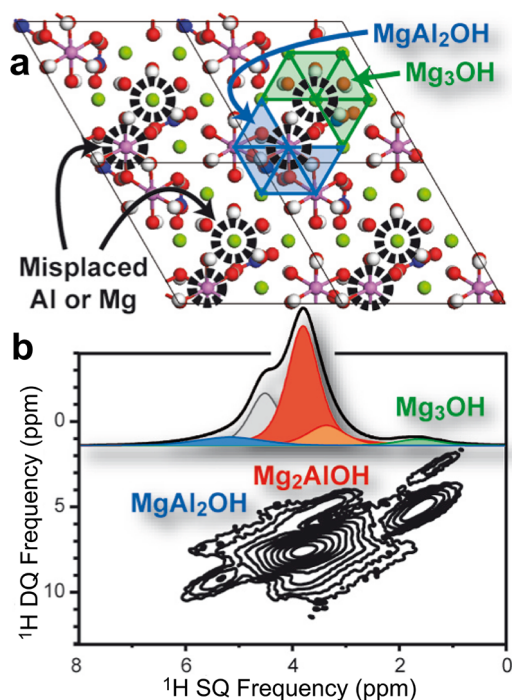


**FIGURE 4.** (a) Top view of one layer of a DFT-optimized model of Mg/Al layered double hydroxide (LDH) with defects introduced in the cation  $\text{Mg}^{2+}/\text{Al}^{3+}$  arrangements. (b) 2D  $^1\text{H}$ - $^1\text{H}$  correlation NMR spectrum probing spatial proximities between protons in LDHs, revealing the presence of additional  $^1\text{H}$  environments characteristic of the defects in the cation distribution.<sup>10</sup>

remained a subject of debate for a long time.<sup>11</sup> This problem was solved by Grey and co-workers<sup>12</sup> using solid-state  $^1\text{H}$  NMR at fast MAS rates and high magnetic fields, a combination of techniques that overcomes the resolution problems that previously limited the use of solid-state  $^1\text{H}$  NMR. In particular, the different types of local structural units resulting from the Mg/Al substitutions were revealed indirectly from the standpoint of nearby hydroxyl groups. Comparisons of the relative populations of the various  $^1\text{H}$  environments ( $\text{Mg}_2\text{AlOH}$ ,  $\text{Mg}_3\text{OH}$ ) as a function of the Mg/Al ratio with different models established that the distribution obeys a law of Al-O-Al avoidance.<sup>13</sup> However, small quantities of Al-O-Al defects are revealed by 2D NMR experiments probing  $^1\text{H}$ - $^1\text{H}$  spatial proximities, which result in enhanced resolution of otherwise overlapping  $^1\text{H}$  contributions (Figure 4).<sup>11</sup>

A similar type of Mg/Al distribution is also present in the octahedral layer 2:1 clays, in which the octahedral layer is sandwiched between two tetrahedral layers composed predominately of  $\text{SiO}_4$  tetrahedra. In this case, the clay sheets exhibit a net negative charge due to the  $\text{Mg}^{2+}$  cations, as opposed to the net positive charge of LDH sheets due to  $\text{Al}^{3+}$  cations. Solid-state  $^1\text{H}$  NMR revealed a principle of

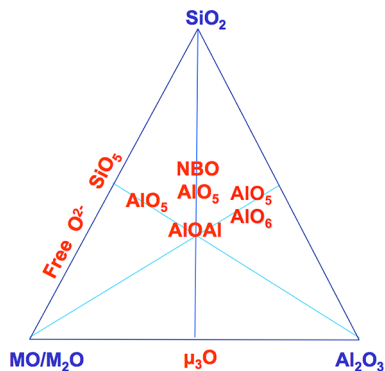


**FIGURE 5.** Unusual coordination states of Si, Al, and O in glasses of ternary  $(\text{MO}/\text{M}_2\text{O})\text{-SiO}_2\text{-Al}_2\text{O}_3$  Systems.<sup>15</sup>

Mg-O-Mg avoidance in synthetic montmorillonite that results, as in LDHs, to a nonrandom cation distribution.<sup>14</sup> These two cases suggest that there may be a general rule of avoidance between charge carriers (whether positive or negative) in the octahedral layers of clays.

### Short-Range Structures in Glasses up to the Nanometer Scale

**Unusual Coordination States.** Even if glasses, or more generally *disordered* materials, are mostly composed of the same building blocks found in crystalline materials, numerous works have shown the presence of low but significant amounts (typically <5%) of unusual atomic coordination states. In ternary aluminosilicate glasses  $(\text{MO}$  or  $\text{M}_2\text{O})\text{-Al}_2\text{O}_3\text{-SiO}_2$  ( $\text{M} = \text{Li}, \text{Na}, \text{K}, \text{Ca},$  or  $\text{Mg}$ ), advanced solid-state NMR experiments have identified the presence of unexpected Si, Al, or O environments that may be characteristic of glasses quenched from high-temperature molten states (Figure 5).

For example, in binary  $(\text{M}_2\text{O}-\text{MO})\text{-SiO}_2$  glasses, Stebbins<sup>16</sup> showed evidence of 5-fold coordinated silicon ( $\text{SiO}_5$ ), already present in small amounts at ambient pressure and favored when glasses are quenched from high pressure.<sup>17</sup> In the per-alkaline domain ( $\text{M}^+ > \text{Al}$  or  $\text{M}^{2+} > 2\text{Al}$ ), despite the large excess of available compensation charges required to stabilize  $\text{AlO}_4$  environments, 5-fold coordinated aluminum atoms ( $\text{AlO}_5$ ) are found throughout the  $\text{CaO-Al}_2\text{O}_3\text{-SiO}_2$  diagram, even at the lowest aluminum content.<sup>18</sup> The formation of these  $\text{AlO}_5$  units is favored at high pressure in the alkali-based glasses.<sup>19,20</sup> For glass compositions located on the charge compensation line ( $\text{M}^+ = \text{Al}$  or  $\text{M}^{2+} = 2\text{Al}$ ), the coexistence of nonbridging oxygen and higher coordination states of aluminum has been established.<sup>19</sup> The presence of  $\mu_3\text{O}$  tricluster O sites, often mentioned in aluminosilicate glasses,<sup>21</sup> has been demonstrated for a  $\text{CaO-Al}_2\text{O}_3$  glass.<sup>22</sup>

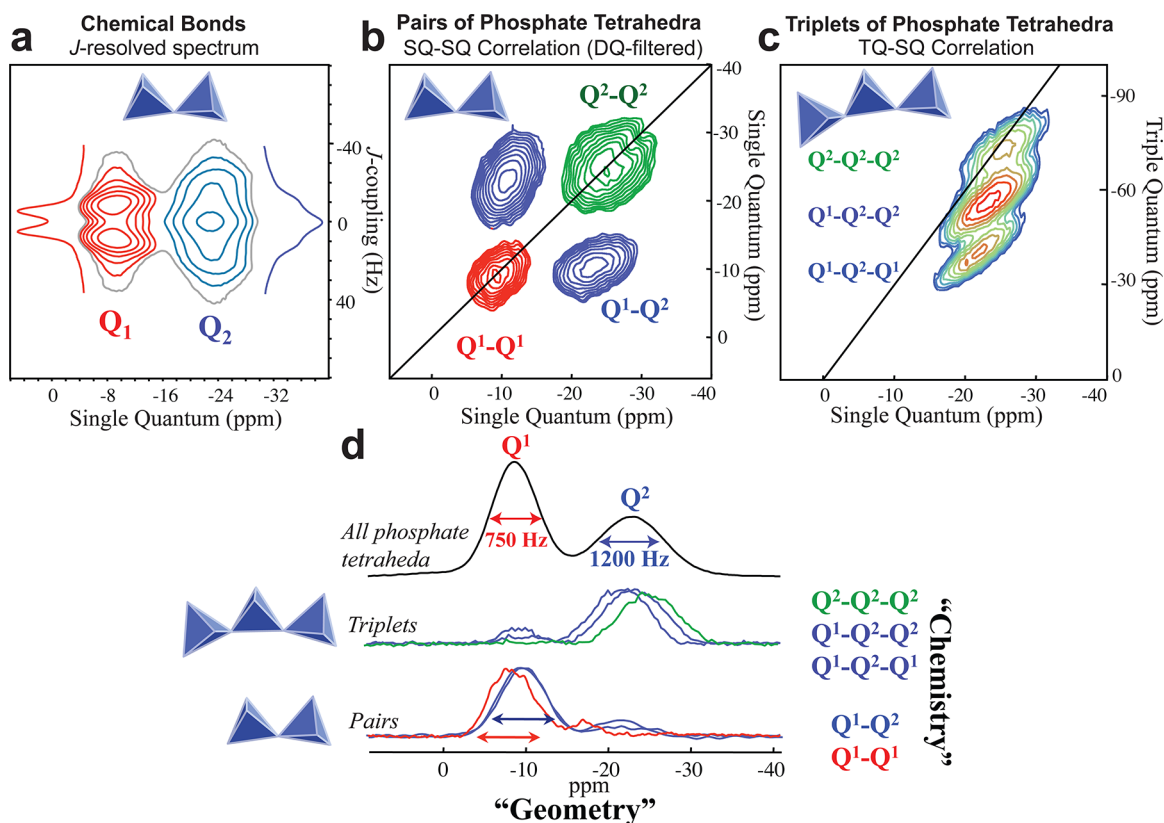


**FIGURE 6.**  $^{31}\text{P}$  NMR characterization of a  $(\text{PbO})_{0.61}(\text{P}_2\text{O}_5)_{0.39}$  glass. (a) Measurements of  $^2J_{\text{P-O-P}}$  couplings. Two-dimensional correlation spectra that select (b) P–P pairs and (c) P–P–P triplets. (d) One-dimensional spectrum reconstructed with the individual quantitative contributions of the different chemical motifs.<sup>25,26</sup>

Similarly, noncoordinated free  $\text{O}^{2-}$  has been observed in binary Ca/Mg silicate glasses.<sup>23,24</sup>

Glasses or amorphous materials thus appear to exhibit a distribution of different chemical environments at the scale of the coordination sphere. However, the question of the glass structure calls for a better description of nanoscale structural units.

**Local Structural Motifs in Phosphate Glasses.** A binary lead phosphate glass of composition  $(\text{PbO})_{0.61}(\text{P}_2\text{O}_5)_{0.39}$  has the stoichiometry of the crystalline  $\text{Pb}_3\text{P}_4\text{O}_{13}$  compound, whose structure consists of tetrameric phosphate units  $\text{Q}^1\text{--Q}^2\text{--Q}^2\text{--Q}^1$  ( $\text{Q} = \text{PO}_4$ ). The  $^{31}\text{P}$  MAS spectrum of this glass sample (Figure 6d) shows two resolved lines assigned from their chemical shifts to  $\text{Q}^1$  and  $\text{Q}^2$  units. The  $\text{Q}^2$  signals are significantly broader than the  $\text{Q}^1$  signals, but their relative integrated signal intensities exhibit a 1:1 ratio, consistent with an average chain length of four tetrahedra observed in the crystalline phase. A measurement of the  $^2J_{\text{P-O-P}}$  couplings (Figure 6a) shows characteristic  $J$ -multiplets: a doublet for the  $\text{Q}^1$  signals (one  $\text{Q}^1\text{--Q}^{x\geq 1}$  bond) and a triplet for the  $\text{Q}^2$  signals (two P–O–P bonds in a  $\text{Q}^{x\geq 1}\text{--Q}^2\text{--Q}^{x\geq 1}$  motif) with associated  $J$ -coupling constants of 17–25 Hz.

A through-bond correlation experiment (Figure 6b) enables the identification of pairs of chemically bonded  $^{31}\text{P}$  nuclei with two autocorrelation lines ( $\text{Q}^1\text{--Q}^1$  corresponding to dimers of phosphate and  $\text{Q}^2\text{--Q}^2$  corresponding to middle of chains) and two cross-correlation lines corresponding to  $\text{Q}^1\text{--Q}^2$  end-of-chain motifs. From this experiment, it appears that the structure of the phosphate network of the glass is composed of phosphate chains with lengths ranging from dimers identified by the  $\text{Q}^1\text{--Q}^1$  line to tetramers or longer chains identified by the  $\text{Q}^2\text{--Q}^2$  chemical bonds. The glass structure thus differs from the structure of the crystalline compound of similar chemical composition by exhibiting a greater diversity of phosphorus chemical environments. We thus unequivocally highlight the variability of local chemical order that is characteristic of the glass structure by identifying structural motifs at the scale of pairs of chemically bonded phosphate units.

To further describe the glass structure, we used a triple-quantum-filtered  $J$ -mediated experiment that selects the signature of the central nucleus of a homonuclear triplet of spins.<sup>26</sup> This experiment (Figure 6c) reveals three different components that can be assigned from their triple-quantum

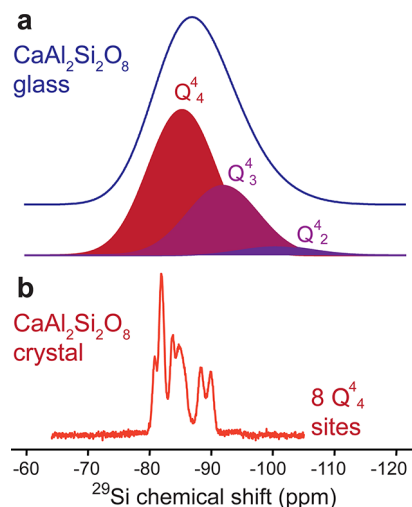


**FIGURE 7.** One-dimensional  $^{29}\text{Si}$  NMR spectra of an anorthite  $\text{CaAl}_2\text{Si}_2\text{O}_8$  (a) glass and (b) crystalline compound with eight distinct  $Q_4^{29}\text{Si}$  sites. The featureless glass spectrum decomposes into  $Q_4^4$ ,  $Q_3^4$ , and  $Q_2^4$  structural motifs that were identified from spin-counting experiments.<sup>11</sup>

resonance frequencies to  $Q^1-Q^2-Q^1$  (phosphate trimers),  $Q^1-Q^2-Q^2$  (end of phosphate tetramers or longer chains), and  $Q^2-Q^2-Q^2$  (middle of phosphate pentamers or longer chains). The use of these multiple-quantum correlation experiments thus enabled five different chemical motifs to be identified at the scale of the coordination sphere of the observed phosphorus: two types of  $Q^1$  environments and three types of  $Q^2$  environments. Considering that the nature and coordination state of the first cationic neighbors of the observed nucleus have been clearly elucidated, the overall size of the identified structural unit approaches the nanometer scale.

Because of the spectral resolution of the different chemical motifs, it is possible to measure for each of them the average chemical shifts and line widths, enabling the quantitative spectrum to be reconstructed and yielding a quantitative interpretation of the structure (Figure 6d). Interestingly, we observe a decreasing chemical shift with increasing polymerization within the  $Q^1$  and  $Q^2$  contributions, as well as between them, and all of the components corresponding to different chemical entities appear to exhibit similar line widths related to their individual geometric disorder. The broader line width observed for the  $Q^2$  signal thus indicates an increased number of locally ordered species.

#### Local Chemical Coordinations in Aluminosilicate Glasses.

The local structures of an aluminosilicate glass of anorthite ( $\text{CaAl}_2\text{Si}_2\text{O}_8$ ) composition can be assessed by a similar NMR approach. The  $^{29}\text{Si}$  MAS spectrum (Figure 7b) of the crystalline phase extends over 10 ppm, with eight different sites of similar chemical environments,  $Q_4^4$ . The  $^{29}\text{Si}$  MAS spectrum of the

corresponding glass (Figure 7a) is broad and featureless, spanning more than 20 ppm, which raises the question of the presence of different  $Q_m^n$  chemical coordinations of  $\text{SiO}_4$  tetrahedra. The through-bond  $^2J_{\text{Si-O-Si}}$  couplings of  $\sim 10$  Hz are small but still strong enough to allow different chemical motifs to be characterized. The  $^{29}\text{Si}$  signal contributions of the different  $Q_m^n$  coordinations can be obtained by modifying the MQ correlation experiment into a MQ-filtered experiment that permits neighboring spins to be counted: while all silicon atoms contribute to the single-quantum spectrum, only pairs of silicon atoms will contribute to the double-quantum-filtered spectrum ( $m \leq 3$ ), triplets to the triple-quantum-filtered spectrum ( $m \leq 2$ ), etc. For a calcium lanthanum yttrium aluminosilicate glass, this method elucidated different  $Q_m^4$  units ranging from  $m = 4$  to  $m = 1$  (up to four quanta filtering).<sup>11</sup> Note that such  $^{29}\text{Si}\{^{29}\text{Si}\}$  MQ experiments require isotopic labeling due to the low natural abundance of  $^{29}\text{Si}$  (4.7%).

For the anorthite glass, we identify quantitatively the different contributions of  $Q_4^4$ ,  $Q_3^4$ , and  $Q_2^4$  chemical motifs by modeling the quantitative 1D  $^{29}\text{Si}$  spectrum using the respective  $Q_m^n$  line shapes obtained from the MQ-filtered experiments (Figure 7a). Note that the fitted width of each chemically different contribution is on the order of 13 ppm, close to the range of  $Q_4^4$  chemical shifts in the crystalline phase, and corresponds to the signature of the geometric disorder of each  $Q_m^4$ . Furthermore, the distribution of  $Q_m^4$  units with  $m < 4$  infers the presence of Al–O–Al bonds and thus confirms the violation of the Lowenstein<sup>8</sup> rule, as already reported from other experiments.<sup>19</sup>

As a summary of the above descriptions of phosphate or aluminosilicate glass structures, taken as prototypes of amorphous structures, we emphasize that the successive identification of individual building units with increasing levels of detail not only can be used to describe their variability but also extends the length scale of our description to a three-dimensional short-range order (up to ca. 1 nm) in solids lacking long-range periodic ordering as measured by diffraction techniques. Forthcoming challenges will be to discuss chain conformations from through-bond experiments and to combine through-bond and through-space experiments to assess the topological relations between extended structural units in three dimensions.

**Nucleation in Glass–Ceramics.** Obtaining a detailed description of extended structural motifs in glass structures is obviously related to the question of the crystallization processes by which glasses may, or may not, convert partly or totally to crystalline phases leading to glass–ceramic composites<sup>27</sup> or dense ceramics.<sup>28</sup> The description of glass

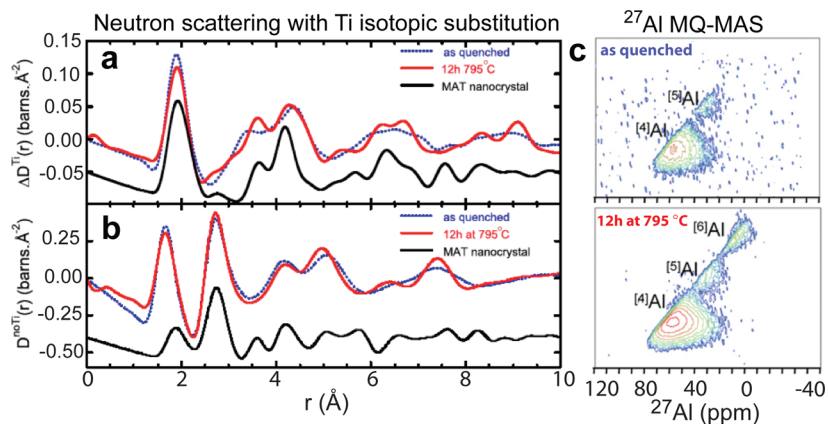


**FIGURE 8.** Combined neutron scattering and  $^{27}\text{Al}$  NMR study of the nucleation process in the glass-ceramic  $2\text{MgO}-2\text{Al}_2\text{O}_3-5\text{SiO}_2$  cordierite system, considering the as-quenched and heat-treated samples:<sup>31</sup> (a) Ti and (b) “Ti-free” pair distribution functions obtained from neutron scattering with Ti isotopic substitution; (c) the  $^{27}\text{Al}$  MQ-MAS NMR spectra.

structures consisting of identified extended structural motifs, possibly involving unusual coordination states, points to the underlying question of how to define and characterize the length and time scales at which chemical and structural homogeneity develop in glasses. If one takes this bias, it is possible to think of the first stages of nucleation in terms of establishing local arrangements that promote crystallization.

The  $2\text{MgO}-2\text{Al}_2\text{O}_3-5\text{SiO}_2$  cordierite system is an archetypal composition in which addition of  $\text{TiO}_2$  is used to promote nucleation for glass–ceramic production. The nucleation process requires the formation of critical clusters from which ordered crystalline structures will grow. However, their characterization is experimentally challenging and welcomes complementary approaches. Neutron scattering with isotopic substitution ( $^{46}\text{Ti}/^{48}\text{Ti}$ ) provides a means to reconstruct “Ti-centered” and “Ti-free” correlation functions (Figure 8a,b), while  $^{27}\text{Al}$  MAS and MQ-MAS NMR allow separation and quantification of the aluminum coordination sites (Figure 8c). The addition of  $\text{TiO}_2$  results in an increasing amount of 5-fold coordinated aluminum; reverse Monte Carlo (RMC) modeling, in combination with neutron and X-ray diffraction and coordination constraints, shows that these highly coordinated aluminum atoms tend to be associated with titanium atoms, approaching the crystalline structure of  $\text{MgTi}_2\text{O}_5-\text{Al}_2\text{TiO}_5$ .<sup>29,30</sup> Upon thermal treatment,<sup>31</sup> Ti-bearing crystals develop, starting from a  $(\text{MgTi}_2\text{O}_5)_{40}-(\text{Al}_2\text{TiO}_5)_{60}$  composition at the cost of  $\text{AlO}_5$  environments in the glass phase (Figure 8) and finally leading to crystallization of cordierite crystals.

## Describing Amorphous Structures As Locally Ordered: A New Paradigm?

Here, we summarize the contributions brought by advanced solid-state NMR techniques to the characterization of the

structure of glasses or, more generally, amorphous materials that do not exhibit long-range order. These materials are generally considered as structurally disordered, without defining the order from which they depart. It is thus difficult to define a parameter that would measure disorder, the definition of which appears to be strongly method dependent. From the local and atom-selective viewpoint of NMR, we propose to describe amorphous or glassy materials as exhibiting well-defined chemical entities at the scale of the coordination sphere and up to the nanometer scale at least. Some of these local arrangements do differ from the canonical structure encountered in most of the related crystalline phases, being energetically unfavored or incompatible with them or preferentially encountered in high-pressure phases (e.g., highly coordinated Si, Al, or O species).

The glass structure thus appears to be a continuous assembly of well-defined local structures reminiscent of the *locally favored structures* introduced by Tanaka and co-workers,<sup>32–34</sup> who further discussed the *dynamic arrest* leading to the glass through fluctuations of structure and dynamics. Those locally favored structures will contribute to the free energy of the system and hence to the positioning of the ensemble structure in the global *energy landscape*. Within this general framework, it is possible to rationalize the difference between the varieties of amorphous structures that can be obtained for the same chemical composition as a function of synthesis conditions. This involves not only the thermal or pressure history (quench rate, etc.) but also the amorphization of crystalline phases.<sup>35,36</sup>

This global description of the glass as an assembly of locally favored structures consisting of a variety of extended structural motifs, possibly involving higher coordination numbers, directly implies chemical and possibly density



heterogeneities down to the nanometer scale. The amorphous structure, macroscopically homogeneous, could thus be described in terms of fluctuations of chemical composition or density related to the local nature of the chemical motifs at a length scale that has to be greater than the nanometer. When the length scale of these fluctuations becomes large enough, such that phase boundaries form, liquid/liquid or glass/glass phase separations occur. This is exemplified by spinodal phase separation, which involves domains of different chemical compositions,<sup>37</sup> or by polyamorphism, which involves phase separation of domains having identical chemical compositions but different densities.<sup>35,38,39</sup>

Remarkably, the study of the progressive incorporation of aluminum in binary CaO–SiO<sub>2</sub><sup>37</sup> shows that there exists a continuous path from the macroscopic spinodal phase separation down to nanometer scale fluctuation of composition. We question the possibility of showing a similar behavior for polyamorphism and fluctuations of density.

## Conclusion

Taking the example of the description of disorder in crystalline structure and extending to the description of nanometer scale structures in oxide glasses and nucleation processes, we have shown how cutting-edge solid-state NMR methods are able to provide detailed insight into the three-dimensional topological, geometric, and chemical order in a variety of solid-state materials. This local approach calls for cooperative benefits from complementary viewpoints obtained (i) experimentally on the average structural description from diffraction or scattering experiments and (ii) *in silico* by reliably predicting NMR parameters from periodic boundary quantum chemistry computations. These results highlight the difficulties in defining a reference ordered state when order and disorder are observed differently from different approaches.

As identified by solid-state NMR, the local structure of amorphous materials or glasses consists of well-identified structural entities up to at least the nanometer scale. Instead of speaking of disorder, we propose a new paradigm to describe their structures in terms of a continuous assembly of locally defined structures, reminiscent of *locally favored structures*<sup>32–34</sup> introduced by Tanaka and co-workers. This draws a comprehensive picture of amorphous structures based on fluctuations of chemical composition and structure over different length scales. We hope that these new local or molecular insights could open new possibilities for considering key questions related to nucleation and crystallization, as well as chemically (e.g., spinodal decomposition) or

density-driven (e.g., polyamorphism) phase separation, which could enable future applications by identifying structure–property relationships.

---

*We gratefully acknowledge financial support from CNRS, TGIR-RMN-THC FR3050, AluBoroSil ANR-09-BLAN-0383-CSD3, and ExaviZ ANR-11-MONU-003. R.J.M. acknowledges support from a Marie Curie Postdoctoral Fellowship through the European Union Seventh Framework Programme (FP7/2007-2013) under Grant Agreement 330735. D.M. acknowledges fruitful discussions with Professors Neville Greaves, Gregory Chass, and Yuanzheng Yue.*

---

## BIOGRAPHICAL INFORMATION

**Dominique Massiot** (Ecole Normale Supérieure - Paris) is the director of the CNRS Institute of Chemistry. He received his thesis in geochemistry from the Université Paris 7 (1983). Working at the CNRS since 1984, he received the CNRS silver medal in 2003. He is the author of ~250 articles on solid-state NMR method development, interpretation, and applications on amorphous materials and glasses.

**Robert Messinger** completed a Ph.D. in chemical engineering from the University of California, Santa Barbara (2012), where his research focused on characterizing and synthesizing hierarchically structured and self-assembled solids and modeling electrokinetic flows and mass transport phenomena. He is currently a Marie Curie Postdoctoral Fellow at the CNRS, where he studies energy materials.

**Sylvian Cadars** received his Ph.D. in chemistry at the Ecole Normale Supérieure (Lyon) in 2006. After a postdoctoral position at University of California, Santa Barbara, U.S.A. (Lavoisier fellow, 2006–2008), he was appointed to a CNRS researcher position in Orléans. His research focuses primarily on the characterization and modeling of hybrid organic–inorganic materials.

**Michaël Deschamps** (Ecole Normale Supérieure - Paris) earned a Ph.D. in chemistry in the group of Geoffrey Bodenhausen in 2001. After an EMBO fellowship at the University of Oxford, he joined CEMHTI laboratory at the CNRS and the Université d'Orléans. He is currently a *Professeur* of chemistry and his research covers NMR methods and applications with a current focus on energy materials.

**Valérie Montouillout** received her Ph.D. in material sciences from the University of Orléans (1998) and entered CNRS as Chargée de Recherches (1999). After 4 years at LCS-CNRS working on catalysis, she joined the CEMHTI laboratory. Her research focuses on the characterization of inorganic materials, especially glasses and crystallization.

**Nadia Pellerin** received her Ph.D. thesis in material sciences from the University of Orléans (1992) and became *Maître de Conférence* in physics. She researches the ageing of glasses under irradiation, leaching, radiolysis, and plasma interaction.

**Emmanuel Véron** received a diploma in chemical physics from Grenoble University (1999) and a Ph.D. in materials sciences at the

University of Orléans (2011). A CNRS engineer since 2001, his research focuses on inorganic compounds characterized by diffraction, electron microscopy, and NMR with application to glass–ceramics for optical applications.

**Mathieu Allix** completed his Ph.D. at the University of Caen (2004). After three years at the University of Liverpool (U.K.), he joined the CNRS (2006). His research covers synthesis and characterization of inorganic materials by electron microscopy and diffraction, focusing on new transparent ceramics.

**Pierre Florian** received an engineer degree from ESEM Orléans and a Ph.D. in physical chemistry at University of Orléans (1993). After 2 years as a postdoctoral researcher at The Ohio State University (U.S.A.), he joined the CNRS in 1996. He currently manages the NMR instruments and his research focuses on developing in situ high-temperature and high-resolution NMR experiments with applications to materials science.

**Franck Fayon** received his Ph.D. thesis in material sciences from the Université d'Orléans (1998) and entered the CNRS as Chargé de Recherche. He is currently director of the CNRS FR2950 federation and his research focuses on the development and application of advanced solid-state NMR methods to biocompatible materials.

#### FOOTNOTES

\*Corresponding author. E-mail: dominique.massiot@cnrs-orleans.fr.  
The authors declare no competing financial interest.

#### REFERENCES

- Lichtenstein, L.; Heyde, M.; Freund, H.-J. Atomic Arrangement in Two-Dimensional Silica: From Crystalline to Vitreous Structures. *J. Phys. Chem. C* **2012**, *116*, 20426–20432.
- Zachariasen, W. H. The Atomic Arrangement in Glass. *J. Am. Chem. Soc.* **1932**, *54*, 3841–3851.
- Krivanek, O. L.; Chisholm, M. F.; Nicolosi, V.; Pennycook, T. J.; Corbin, G. J.; Dellby, N.; Murfitt, M. F.; Own, C. S.; Szilagyi, Z. S.; Oxley, M. P.; Pantelides, S. T.; Pennycook, S. J. Atom-by-Atom Structural and Chemical Analysis by Annular Dark-Field Electron Microscopy. *Nature* **2010**, *464*, 571–574.
- Greaves, G. N. EXAFS and the Structure of Glass. *J. Non-Cryst. Solids* **1985**, *71*, 203–217.
- Florian, P.; Véron, E.; Green, T.; Yates, J. R.; Massiot, D. Elucidation of the Al/Si Ordering in Gehlenite  $\text{Ca}_2\text{Al}_2\text{SiO}_7$  by Combined  $^{29}\text{Si}$  and  $^{27}\text{Al}$  NMR Spectroscopy/Quantum Chemical Calculations. *Chem. Mater.* **2012**, *24*, 4068–4079.
- Lejus, A. M.; Pelletier Allard, N.; Pelletier, R.; Vivien, D. Site Selective Spectroscopy of Nd Ions in Gehlenite ( $\text{Ca}_2\text{Al}_2\text{SiO}_7$ ), a New Laser Material. *Opt. Mater.* **1996**, *6*, 129–137.
- Kimata, M.; Ii, N. The Structural Property of Synthetic Gehlenite,  $\text{Ca}_2\text{Al}_2\text{SiO}_7$ . *Neues Jahrb. Mineral., Abh.* **1982**, *144*, 254–267.
- Loewenstein, W. The Distribution of Aluminum in the Tetrahedra of Silicates and Aluminates. *Am. Mineral.* **1954**, *39*, 92–96.
- Véron, E.; Garaga, M. N.; Pelloquin, D.; Cadars, S.; Suchomel, M.; Suard, E.; Massiot, D.; Montouillout, V.; Matzen, G.; Allix, M. Synthesis and Structure Determination of  $\text{CaSi}_{1/3}\text{B}_{2/3}\text{O}_{8/3}$ : A New Calcium Borosilicate. *Inorg. Chem.* **2013**, *52*, 4250–4258.
- Cadars, S.; Layrac, G.; Gérardin, C.; Deschamps, M.; Yates, J. R.; Tichit, D.; Massiot, D. Identification and Quantification of Defects in the Cation Ordering in Mg/Al Layered Double Hydroxides. *Chem. Mater.* **2011**, *23*, 2821–2831 and references therein.
- Hiet, J.; Deschamps, M.; Pellerin, N.; Fayon, F.; Massiot, D. Probing Chemical Disorder in Glasses Using Silicon-29 NMR Spectral Editing. *Phys. Chem. Chem. Phys.* **2009**, *11*, 6935–6940.
- Sideris, P. J.; Nielsen, U. G.; Gan, Z. H.; Grey, C. P. Mg/Al Ordering in Layered Double Hydroxides Revealed by Multinuclear NMR Spectroscopy. *Science* **2008**, *321*, 113–117.
- Sideris, P. J.; Blanc, F.; Gan, Z.; Grey, C. P. Identification of Cation Clustering in Mg–Al Layered Double Hydroxides Using Multinuclear Solid State Nuclear Magnetic Resonance Spectroscopy. *Chem. Mater.* **2012**, *24*, 2449–2461.
- Cadars, S.; Guégan, R.; Garaga, M. N.; Bourrat, X.; Le Forestier, L.; Fayon, F.; Huynh, T. V.; Allier, T.; Nour, Z.; Massiot, D. New Insights into the Molecular Structures, Compositions, and Cation Distributions in Synthetic and Natural Montmorillonite Clays. *Chem. Mater.* **2012**, *24*, 4376–4389.
- Massiot, D.; Fayon, F.; Montouillout, V.; Pellerin, N.; Hiet, J.; Roiland, C.; Florian, P.; Coutures, J. P.; Cormier, L.; Neuville, D. R. Structure and Dynamics of Oxide Melts and Glasses: A View from Multinuclear and High Temperature NMR. *J. Non-Cryst. Solids* **2008**, *354*, 249–254.
- Stebbins, J. F. NMR Evidence for Five-Coordinated Silicon in a Silicate Glass at Atmospheric Pressure. *Nature* **1991**, *351*, 638–639.
- Allwardt, J. R.; Schmidt, B. C.; Stebbins, J. F. Structural Mechanisms of Compression and Decompression in High-Pressure  $\text{K}_2\text{Si}_4\text{O}_9$  Glasses: An Investigation Utilizing Raman and NMR Spectroscopy of Glasses and Crystalline Materials. *Chem. Geol.* **2004**, *213*, 137–151.
- Neuville, D. R.; Cormier, L.; Massiot, D. Al Coordination and Speciation in Calcium Aluminosilicate Glasses: Effects of Composition Determined by  $^{27}\text{Al}$  MQ-MAS NMR and Raman Spectroscopy. *Chem. Geol.* **2006**, *229*, 173–185.
- Stebbins, J. F.; Xu, Z. NMR Evidence for Excess Non-bridging Oxygen in an Aluminosilicate Glass. *Nature* **1997**, *390*, 60–62.
- Allwardt, J. R.; Stebbins, J. F.; Schmidt, B. C.; Frost, D. J.; Withers, A. C.; Hirschmann, M. M. Aluminum Coordination and the Densification of High-Pressure Aluminosilicate Glasses. *Am. Mineral.* **2005**, *90*, 1218–1222.
- Toplis, M. J.; Dingwell, D. B.; Lenci, T. Peraluminous Viscosity Maxima in  $\text{Na}_2\text{O}$ – $\text{Al}_2\text{O}_3$ – $\text{SiO}_2$  Liquids: The Role of Triclusters in Tectosilicate Melts. *Geochim. Cosmochim. Acta* **1997**, *61*, 2605–2612.
- Iuga, D.; Morais, C. M.; Gan, Z.; Neuville, D. R.; Cormier, L.; Massiot, D. NMR Heteronuclear Correlation between Quadrupolar Nuclei in Solids. *J. Am. Chem. Soc.* **2005**, *127*, 11540–11541.
- Nasikas, N. K.; Chrissanthopoulos, A.; Bouropoulos, N.; Sen, S.; Papatheodorou, G. N. Silicate Glasses at the Ionic Limit: Alkaline-Earth Sub-Orthosilicates. *Chem. Mater.* **2011**, *23*, 3692–3697.
- Nasikas, N. K.; Edwards, T. G.; Sen, S.; Papatheodorou, G. N. Structural Characteristics of Novel Ca–Mg Orthosilicate and Suborthosilicate Glasses: Results from  $^{29}\text{Si}$  and  $^{17}\text{O}$  NMR Spectroscopy. *J. Phys. Chem. B* **2012**, *116*, 2696–2702.
- Fayon, F.; King, I. J.; Harris, R. K.; Evans, J. S. O.; Massiot, D. Application of the through-Bond NMR Correlation Experiment to the Characterization of Crystalline and Disordered Phosphates. *C. R. Chim.* **2004**, *7*, 351–361.
- Fayon, F.; Roiland, C.; Emsley, L.; Massiot, D. Triple-quantum Correlation NMR Experiments in Solids Using J-Couplings. *J. Magn. Reson.* **2006**, *179*, 50–58.
- McMillan, P. W. *Glass–Ceramics*; Academic Press: London and New York, 1979.
- Allix, M.; Alahrache, S.; Fayon, F.; Suchomel, M.; Porcher, F.; Cardinal, T.; Matzen, G. Highly Transparent  $\text{BaAl}_4\text{O}_7$  Polycrystalline Ceramic Obtained by Full Crystallization from Glass. *Adv. Mater.* **2012**, *24*, 5570–5575.
- Guignard, M.; Cormier, L.; Montouillout, V.; Menguy, N.; Massiot, D.; Hannon, A. C. Environment of Titanium and Aluminium in a Magnesium Aluminosilicate Glass. *J. Phys.: Condens. Matter* **2009**, *21*, No. 375107.
- Guignard, M.; Cormier, L.; Montouillout, V.; Menguy, N.; Massiot, D. Structural Fluctuations and Role of Ti as Nucleating Agent in an Aluminosilicate Glass. *J. Non-Cryst. Solids* **2010**, *356*, 1368–1373.
- Guignard, M.; Cormier, L.; Montouillout, V.; Menguy, N.; Massiot, D.; Hannon, A. C.; Beuneu, B. Rearrangement of the Structure during Nucleation of a Cordierite Glass Doped with  $\text{TiO}_2$ . *J. Phys.: Condens. Matter* **2010**, *22*, No. 185401.
- Kawasaki, T.; Araki, T.; Tanaka, H. Correlation between Dynamic Heterogeneity and Medium-Range Order in Two-Dimensional Glass-Forming Liquids. *Phys. Rev. Lett.* **2007**, *99*, No. 215701.
- Royall, C. P.; Williams, S. R.; Ohtsuka, T.; Tanaka, H. Direct Observation of a Local Structural Mechanism for Dynamic Arrest. *Nat. Mater.* **2008**, *7*, 556–561.
- Tanaka, H.; Kawasaki, T.; Shintani, H.; Watanabe, K. Critical-like Behaviour of Glass-Forming Liquids. *Nat. Mater.* **2010**, *9*, 324–331.
- Greaves, G. N.; Meneau, F.; Majerus, O.; Jones, D. G.; Taylor, J. Identifying Vibrations That Destabilize Crystals and Characterize the Glassy State. *Science* **2005**, *308*, 1299–1302.
- Greaves, G. N.; Meneau, F.; Kargl, F.; Ward, D.; Holliman, P.; Albergamo, F. Zeolite Collapse and Polyamorphism. *J. Phys.: Condens. Matter* **2007**, *19*, No. 415102.
- Martel, L.; Allix, M.; Millot, F.; Sarou-Kanian, V.; Véron, E.; Ory, S.; Massiot, D.; Deschamps, M. Controlling the Size of Nanodomains in Calcium Aluminosilicate Glasses. *J. Phys. Chem. C* **2011**, *115*, 18935–18945.
- Poole, P. H.; Grande, T.; Angell, C. A.; McMillan, P. F. Polymorphic Phase Transitions in Liquids and Glasses. *Science* **1997**, *275*, 322–323.
- Greaves, G. N.; Wilding, M. C.; Feam, S.; Langstaff, D.; Kargl, F.; Cox, S.; Vu Van, Q.; Majerus, O.; Benmore, C. J.; Weber, R.; Martin, C. M.; Hennet, L. Detection of First Order Liquid–Liquid Phase Transitions in Yttrium Oxide–Aluminium Oxide Melts. *Science* **2008**, *322*, 566–570.